Multi-scale Finite Element Method for incompressible flow

Loïc Balazi [1,2] (loic.balazi@polytechnique.edu)
G. Allaire [2] P. Omnes [1]

[1]SGLS, CEA Saclay
[2]CMAP, Ecole Polytechnique

FreeFEM Days 2023, LJLL
7–8 december 2023

Sommaire

Multi-scale problems are ubiquitous

Soil

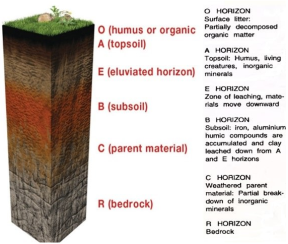

Composite Materials

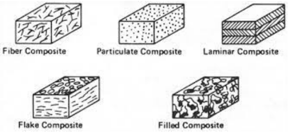

Airflow in a dense city

Multi-scale problems are ubiquitous

Nuclear reactor core : a multi-scale medium with many obstacles.

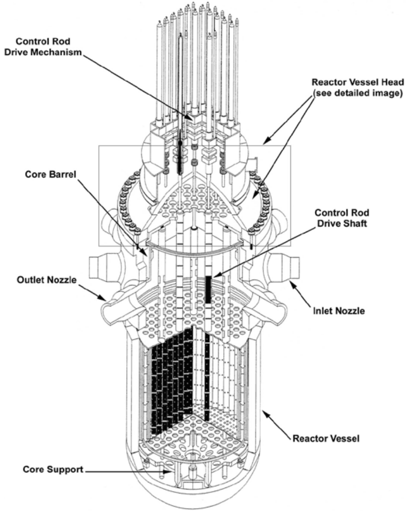

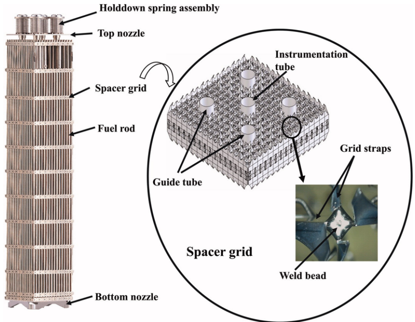

PWR Fuel assembly

Model Problem

- We define a perforated domain $\Omega^\varepsilon \subset \mathbb{R}^d$ ($d = 2, 3$) as :

$$\Omega^\varepsilon = \Omega \setminus B^\varepsilon \tag{1}$$

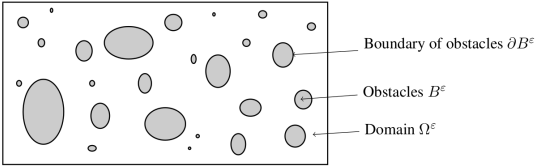

Figure: Rectangular domain Ω comprising a fluid domain Ω^ε perforated by a set of obstacles B^ε

Model Problem

- We define a perforated domain $\Omega^\varepsilon \subset \mathbb{R}^d$ $(d = 2, 3)$ as :

$$\Omega^\varepsilon = \Omega \setminus B^\varepsilon \tag{1}$$

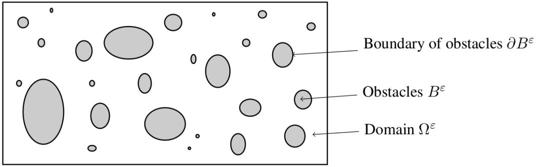

Figure: Rectangular domain Ω comprising a fluid domain Ω^ε perforated by a set of obstacles B^ε

- **Goal** : Solve the Navier-**Stokes** equations in Ω^ε : Find the velocity $\boldsymbol{u}_\varepsilon : \Omega^\varepsilon \to \mathbb{R}^d$ and the pressure $p_\varepsilon : \Omega^\varepsilon \to \mathbb{R}$ to :

$$\left\{\begin{array}{rclll} \partial_t \boldsymbol{u}_\varepsilon - \nu \Delta \boldsymbol{u}_\varepsilon + \boldsymbol{u}_\varepsilon \cdot \boldsymbol{\nabla} \boldsymbol{u}_\varepsilon + \boldsymbol{\nabla} p_\varepsilon & = & \boldsymbol{f} & \text{in} & \Omega^\varepsilon \\ \text{div } \boldsymbol{u}_\varepsilon & = & 0 & \text{in} & \Omega^\varepsilon \\ \boldsymbol{u}_\varepsilon & = & \boldsymbol{0} & \text{on} & \partial B^\varepsilon \cap \partial \Omega^\varepsilon \\ \boldsymbol{u}_\varepsilon & = & \boldsymbol{g} & \text{on} & \partial \Omega \cap \partial \Omega^\varepsilon \\ \boldsymbol{u}_\varepsilon(t=0) & = & u_0 & \text{in} & \Omega^\varepsilon \end{array}\right. \tag{2}$$

Motivations of MsFEM

- Assume we discretize the Stokes equations (2) using classical Crouzeix-Raviart Finite Element [1], then the relative error bound is given by :

$$\frac{1}{|u_\varepsilon|_{H^1(\Omega)}}\left(|u_\varepsilon - u_H|_{H,1} + \|p_\varepsilon - p_H\|_{L^2(\Omega)}\right) \leq CH \underbrace{\left(|u_\varepsilon|_{H^2(\Omega)} + |p_\varepsilon|_{H^1(\Omega)}\right)\frac{1}{|u_\varepsilon|_{H^1(\Omega)}}}_{\beta_\varepsilon} \quad (3)$$

Since $\beta_\varepsilon \approx \frac{1}{\varepsilon}$, this leads to requiring $H \ll \varepsilon \Rightarrow$ **Too expensive**.

Motivations of MsFEM

- Assume we discretize the Stokes equations (2) using classical Crouzeix-Raviart Finite Element [1], then the relative error bound is given by :

$$\frac{1}{|u_\varepsilon|_{H^1(\Omega)}}\left(|u_\varepsilon - u_H|_{H,1} + \|p_\varepsilon - p_H\|_{L^2(\Omega)}\right) \leq CH \underbrace{\left(|u_\varepsilon|_{H^2(\Omega)} + |p_\varepsilon|_{H^1(\Omega)}\right)\frac{1}{|u_\varepsilon|_{H^1(\Omega)}}}_{\beta_\varepsilon} \qquad (3)$$

  Since $\beta_\varepsilon \approx \frac{1}{\varepsilon}$, this leads to requiring $H \ll \varepsilon \Rightarrow$ **Too expensive**.
- Several numerical multi-scale approaches :
  - Heterogeneous Multi-scale Methods (HMM) [2, 3, 4]
  - Local Orthogonal Decomposition (LOD) [5]
  - etc, ...

Motivations of MsFEM

- Assume we discretize the Stokes equations (2) using classical Crouzeix-Raviart Finite Element [1], then the relative error bound is given by :

$$\frac{1}{|u_\varepsilon|_{H^1(\Omega)}}\left(|u_\varepsilon - u_H|_{H,1} + \|p_\varepsilon - p_H\|_{L^2(\Omega)}\right) \leq CH \underbrace{\left(|u_\varepsilon|_{H^2(\Omega)} + |p_\varepsilon|_{H^1(\Omega)}\right)\frac{1}{|u_\varepsilon|_{H^1(\Omega)}}}_{\beta_\varepsilon} \quad (3)$$

  Since $\beta_\varepsilon \approx \frac{1}{\varepsilon}$, this leads to requiring $H \ll \varepsilon \Rightarrow$ **Too expensive**.
- Several numerical multi-scale approaches :
  - Heterogeneous Multi-scale Methods (HMM) [2, 3, 4]
  - Local Orthogonal Decomposition (LOD) [5]
  - etc, ...

Motivations of MsFEM

- Assume we discretize the Stokes equations (2) using classical Crouzeix-Raviart Finite Element [1], then the relative error bound is given by :

$$\frac{1}{|u_\varepsilon|_{H^1(\Omega)}}\left(|u_\varepsilon - u_H|_{H,1} + \|p_\varepsilon - p_H\|_{L^2(\Omega)}\right) \leq CH \underbrace{\left(|u_\varepsilon|_{H^2(\Omega)} + |p_\varepsilon|_{H^1(\Omega)}\right)\frac{1}{|u_\varepsilon|_{H^1(\Omega)}}}_{\beta_\varepsilon} \quad (3)$$

Since $\beta_\varepsilon \approx \frac{1}{\varepsilon}$, this leads to requiring $H \ll \varepsilon \Rightarrow$ **Too expensive**.

- Several numerical multi-scale approaches :
  - Heterogeneous Multi-scale Methods (HMM) [2, 3, 4]
  - Local Orthogonal Decomposition (LOD) [5]
  - etc, ...
- **Multi-scale Finite Element Method (MsFEM)**

Sommaire

Main idea of MsFEM

- Solving a global problem (defined on a coarse mesh) using a Galerkin approximation $\mathcal{A}_{glob}(u_H, v) = \ell_{glob}(v)$

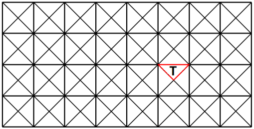

Main idea of MsFEM

- Solving a global problem (defined on a coarse mesh) using a Galerkin approximation $\mathcal{A}_{glob}(u_H, v) = \ell_{glob}(v)$

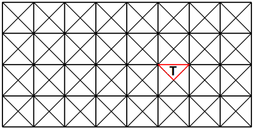

- Basis functions **no longer classical Lagrange polynomial** : $\mathcal{P}_1, \mathcal{P}_2, \ldots, \mathcal{P}_n$.

Main idea of MsFEM

- Solving a global problem (defined on a coarse mesh) using a Galerkin approximation $\mathcal{A}_{glob}(u_H, v) = \ell_{glob}(v)$

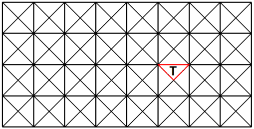

- Basis functions **no longer classical Lagrange polynomial** : $\cancel{\mathcal{P}_1}, \cancel{\mathcal{P}_2}, \ldots, \cancel{\mathcal{P}_n}$.

Main idea of MsFEM

- Solving a global problem (defined on a coarse mesh) using a Galerkin approximation $\mathcal{A}_{glob}(u_H, v) = \ell_{glob}(v)$

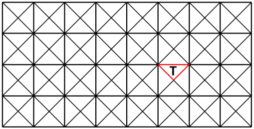

- Basis functions **no longer classical Lagrange polynomial** : $\cancel{\mathcal{P}_1}, \cancel{\mathcal{P}_2}, \dots, \cancel{\mathcal{P}_n}$.
- <u>But</u> **suitably chosen local basis functions** that solve $\mathcal{A}_{loc}(\Phi_h, v) = \ell_{loc}(v)$ and which :
  - Depend on the physics computed ;
  - Encode the obstacles or other local heterogeneity ;
  - Do not depend on the load $\boldsymbol{f}$ and the boundary conditions $\boldsymbol{g}$.

Main idea of MsFEM

- Solving a global problem (defined on a coarse mesh) using a Galerkin approximation $\mathcal{A}_{glob}(u_H, v) = \ell_{glob}(v)$

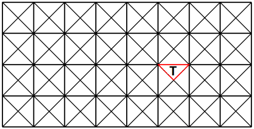

- Basis functions **no longer classical Lagrange polynomial** : $\cancel{\mathcal{P}_1}, \cancel{\mathcal{P}_2}, \ldots, \cancel{\mathcal{P}_n}$.
- But **suitably chosen local basis functions** that solve $\mathcal{A}_{loc}(\Phi_h, v) = \ell_{loc}(v)$ and which :
  - Depend on the physics computed ;
  - Encode the obstacles or other local heterogeneity ;
  - Do not depend on the load $\boldsymbol{f}$ and the boundary conditions $\boldsymbol{g}$.
- Particularly worthwhile in a multi-query context : need to solve the global problem for several loads $\boldsymbol{f}$ and boundary conditions $\boldsymbol{g}$.

MsFEM Algorithm

- Partition the domain into a set of coarse elements (coarse mesh)
- For each coarse element (**In parallel**) **(offline phase = expensive)** :
  - Partition the element into a fine mesh
  - Construct multi-scale basis functions (local problems) $\Rightarrow$ **In parallel**
  - Compute matrices locally on the fine mesh
- Assemble global matrices and solve the coarse-scale problem **(online phase = cheap)**
- For each coarse element **In parallel**:
  - Reconstruct fine-scale solutions on the fine mesh

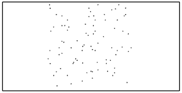

(a) heterogeneous domain Ω^{ε}

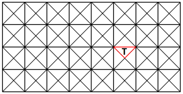

(b) coarse mesh $\mathcal{T}_H$ and element T

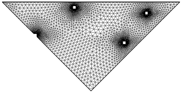

(c) fine mesh $\mathcal{T}_h(T)$

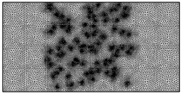

(d) reference mesh $\mathcal{T}_h(\Omega^{\varepsilon})$

General strategy to find a MsFEM space

Assume the variational formulation of the original problem reads :

$$\text{Find } u \in V \ s.t \ a(u, v) = \ell(v) \quad \forall v \in V \tag{4}$$

The idea is to decompose $u = u_H + u_0$, with $u_H \in V_H$ the space of the "resolved parts" and $u_0 \in V_0$ the space of the "unresolved parts". Then

$$a(u, v) = a(u_H, v_H) + a(u_0, v_H) = \ell(v_H), \quad \forall v_H \in V_H \tag{5}$$

If $a(u_0, v_H) = 0$ then we can "forget" the unresolved part u_0 and solve for the resolved part u_H through:

$$\text{Find } u_H \in V_H \ s.t \ a(u_H, v_H) = \ell(v_H), \quad \forall v_H \in V_H \tag{6}$$

provided this problem has a (unique) solution.

Sommaire

Stokes Problem : Setting

- Variational formulation : Find $(\boldsymbol{u}_{\boldsymbol{\varepsilon}}, p_\varepsilon) \in X$ such that :

$$c\left((\boldsymbol{u}_{\boldsymbol{\varepsilon}}, p_\varepsilon), (\boldsymbol{v}, q)\right) = \int_{\Omega^\epsilon} \boldsymbol{f} \cdot \boldsymbol{v}, \qquad \forall (\boldsymbol{v}, q) \in X, \tag{7}$$

where the bi-linear form c is defined by :

$$c\left((\boldsymbol{u}_{\boldsymbol{\varepsilon}}, p_\varepsilon), (\boldsymbol{v}, q)\right) = \int_{\Omega^\epsilon} \left(\nu \boldsymbol{\nabla} \boldsymbol{u}_{\boldsymbol{\varepsilon}} : \boldsymbol{\nabla} \boldsymbol{v} - p_\varepsilon \ \mathrm{div}\ \boldsymbol{v} - q \ \mathrm{div}\ \boldsymbol{u}_{\boldsymbol{\varepsilon}}\right) \tag{8}$$

Stokes Problem : Setting

- Variational formulation : Find $(\boldsymbol{u_\varepsilon}, p_\varepsilon) \in X$ such that :

$$c\left((\boldsymbol{u_\varepsilon}, p_\varepsilon), (\boldsymbol{v}, q)\right) = \int_{\Omega^\epsilon} \boldsymbol{f} \cdot \boldsymbol{v}, \qquad \forall (\boldsymbol{v}, q) \in X, \tag{7}$$

where the bi-linear form c is defined by :

$$c\left((\boldsymbol{u_\varepsilon}, p_\varepsilon), (\boldsymbol{v}, q)\right) = \int_{\Omega^\epsilon} \left(\nu \boldsymbol{\nabla} \boldsymbol{u_\varepsilon} : \boldsymbol{\nabla} \boldsymbol{v} - p_\varepsilon \ \mathrm{div}\ \boldsymbol{v} - q \ \mathrm{div}\ \boldsymbol{u_\varepsilon}\right) \tag{8}$$

and the classical spaces are defined by :

$$X = V \times M \tag{9}$$

$$V = H_0^1(\Omega^\varepsilon)^d = \{u \in H^1(\Omega^\varepsilon) : u|_{\partial\Omega^\varepsilon = 0}\} \text{ for the velocity,} \tag{10}$$

and

$$M = L_0^2(\Omega^\varepsilon) = \{p \in L^2(\Omega^\varepsilon) \ s.t \ \int_{\Omega^\varepsilon} p = 0\} \text{ for the pressure.} \tag{11}$$

Stokes Problem : Setting

- Variational formulation : Find $(\boldsymbol{u}_{\varepsilon}, p_{\varepsilon}) \in X$ such that :

$$c\left((\boldsymbol{u}_{\varepsilon}, p_{\varepsilon}), (\boldsymbol{v}, q)\right) = \int_{\Omega^{\epsilon}} \boldsymbol{f} \cdot \boldsymbol{v}, \qquad \forall (\boldsymbol{v}, q) \in X, \tag{7}$$

where the bi-linear form c is defined by :

$$c\left((\boldsymbol{u}_{\varepsilon}, p_{\varepsilon}), (\boldsymbol{v}, q)\right) = \int_{\Omega^{\epsilon}} \left(\nu \boldsymbol{\nabla} \boldsymbol{u}_{\varepsilon} : \boldsymbol{\nabla} \boldsymbol{v} - p_{\varepsilon} \ \operatorname{div} \boldsymbol{v} - q \ \operatorname{div} \boldsymbol{u}_{\varepsilon}\right) \tag{8}$$

and the classical spaces are defined by :

$$X = V \times M \tag{9}$$

$$V = H_0^1(\Omega^{\varepsilon})^d = \{u \in H^1(\Omega^{\varepsilon}) : u|_{\partial\Omega^{\varepsilon}=0}\} \text{ for the velocity,} \tag{10}$$

and

$$M = L_0^2(\Omega^{\varepsilon}) = \{p \in L^2(\Omega^{\varepsilon}) \ s.t \int_{\Omega^{\varepsilon}} p = 0\} \text{ for the pressure.} \tag{11}$$

Step 1 : Extended velocity space

To build the approximation spaces of enriched Crouzeix-Raviart MsFEM, we define V_H^{ext} (non-conforming FE space) :

$$V_H^{ext} = \left\{ \begin{array}{l} \boldsymbol{u_\varepsilon} \in (L^2(\Omega^\varepsilon))^d \ s.t \ \boldsymbol{u_\varepsilon}|_T \in (H^1(T \cap \Omega^\varepsilon))^d \text{ for any } T \in \mathcal{T}_H, \\ \boldsymbol{u_\varepsilon} = \mathbf{0} \text{ on } \partial B^\varepsilon, \displaystyle\int_{E \cap \partial\Omega^\varepsilon} [[\boldsymbol{u_\varepsilon}]] \cdot \boldsymbol{\omega_{E,i}} = 0 \text{ for all } E \in \mathcal{E}_H, i = 1, \dots, s \end{array} \right\} \tag{12}$$

where $(\boldsymbol{\omega_{E,i}})_{1 \le i \le s}$ is a set of basis functions of $(\mathbb{P}_n(E))^d$ and $s = \dim(\mathbb{P}_n(E)^d)$.
The extended velocity-pressure space is defined as :

$$X_H^{ext} = V_H^{ext} \times M \tag{13}$$

Step 1 : Extended velocity space

To build the approximation spaces of enriched Crouzeix-Raviart MsFEM, we define V_H^{ext} (non-conforming FE space) :

$$V_H^{ext} = \left\{ \begin{array}{l} \boldsymbol{u_\varepsilon} \in (L^2(\Omega^\varepsilon))^d \ s.t \ \boldsymbol{u_\varepsilon}|_T \in (H^1(T \cap \Omega^\varepsilon))^d \text{ for any } T \in \mathcal{T}_H, \\ \boldsymbol{u_\varepsilon} = \mathbf{0} \text{ on } \partial B^\varepsilon, \displaystyle\int_{E \cap \partial\Omega^\varepsilon} [[\boldsymbol{u_\varepsilon}]] \cdot \boldsymbol{\omega_{E,i}} = 0 \text{ for all } E \in \mathcal{E}_H, i = 1, \ldots, s \end{array} \right\} \tag{12}$$

where $(\boldsymbol{\omega_{E,i}})_{1 \le i \le s}$ is a set of basis functions of $(\mathbb{P}_n(E))^d$ and $s = \dim(\mathbb{P}_n(E)^d)$.
The extended velocity-pressure space is defined as :

$$X_H^{ext} = V_H^{ext} \times M \tag{13}$$

Decomposition of the FE space

We want to decompose X_H^{ext} into a direct sum of a finite dimensional subspace X_H (resolved coarse scales) and an infinite dimensional subspace X_H^0 (unresolved fine scales) :

$$X_H^{ext} = X_H \oplus X_H^0, \tag{14}$$

Step 2 : Choice of the unresolved space X_H^0

Definition (Infinite dimensional space X_H^0)

The velocity-pressure space X_H^0 is defined as a subspace of X_H^{ext} by :

$$X_H^0 = V_H^0 \times M_H^0, \quad \textit{with}$$

$$V_H^0 = \left\{ \begin{array}{l} \boldsymbol{u_\varepsilon} \in V_H^{ext} \ s.t \displaystyle\int_{E \cap \Omega^\varepsilon} \boldsymbol{u_\varepsilon} \cdot \boldsymbol{\omega_{E,j}} = 0, \int_{T \cap \Omega^\varepsilon} \boldsymbol{u_\varepsilon} \cdot \boldsymbol{\varphi_{T,k}} = 0, \\ \forall T \in \mathcal{T}_H, \forall E \in \mathcal{E}_H, j = 1, \dots, s, k = 1, \dots, r. \end{array} \right\} \tag{15}$$

and

$$M_H^0 = \left\{ p \in M \ s.t \int_{T \cap \Omega^\varepsilon} p \varpi_{T,j} = 0, \forall T \in \mathcal{T}_H, j = 1, \dots, t \right\} \tag{16}$$

- $(\boldsymbol{\omega_{E,i}})_{1 \leq i \leq s}$ is a set of basis functions of $(\mathbb{P}_n(E))^d$ and $s = \dim(\mathbb{P}_n(E)^d)$
- $(\boldsymbol{\varphi_{T,k}})_{1 \leq k \leq r}$ is a set of basis functions of $(\mathbb{P}_{n-1}(T))^d$ and $r = \dim(\mathbb{P}_{n-1}(T)^d)$
- $(\varpi_{T,j})_{1 \leq j \leq t}$ is a set of basis functions of $\mathbb{P}_n(T)$ and $t = \dim(\mathbb{P}_n(T))$

Step 3 : Determine the resolved space X_H

Definition (Finite dimensional subspace X_H)

The velocity-pressure space X_H is defined as a subspace of X_H^{ext}, being the **"orthogonal"** complement of X_H^0 with respect to the bilinear form c_H as follows:

$$(\boldsymbol{u_H}, p_H) \in X_H \iff \begin{array}{l} (\boldsymbol{u_H}, p_H) \in X_H^{ext} \textit{ such that} \\ c_H((\boldsymbol{u_H}, p_H), (\boldsymbol{v}, q)) = 0, \forall (\boldsymbol{v}, q) \in X_H^0 \end{array} \tag{17}$$

where c_H is defined by

$$c_H((\boldsymbol{u_H}, p_H), (\boldsymbol{v}, q)) = \sum_{T \in \mathcal{T}_H} \int_{T \cap \Omega^\varepsilon} (\mu \boldsymbol{\nabla} \boldsymbol{u_H} : \boldsymbol{\nabla} \boldsymbol{v} - p_H \ \mathrm{div}\ \boldsymbol{v} - q \ \mathrm{div}\ \boldsymbol{u_H}).$$

Characterisation of the resolved space X_H

The resolved space is defined by :

$$X_H = V_H \times M_H.$$

Theorem (Space M_H)

$$M_H = \{q \in M \text{ such that } q|_T \in \mathbb{P}_n(T),\ \forall\ T \in \mathcal{T}_H\} \tag{18}$$

which corresponds to a fully discontinuous polynomial of order n.

Theorem (Basis of the space V_H)

$$V_H = \mathrm{span}\{\boldsymbol{\Phi}\} \tag{19}$$

with

$$\boldsymbol{\Phi} = \underbrace{\left(\bigcup_{E \in \mathcal{E}_H, i} \boldsymbol{\Phi}_{\boldsymbol{E},\boldsymbol{i}}\right)}_{\textit{Face basis functions}} \cup \underbrace{\left(\bigcup_{T \in \mathcal{T}_H, k} \boldsymbol{\Psi}_{\boldsymbol{T},\boldsymbol{k}}\right)}_{\textit{Element basis functions}} \tag{20}$$

Definition of basis functions

■ **Basis functions associated to faces of the coarse mesh** : For any $E \in \mathcal{E}_H$, for $i = 1, \ldots, s$, find the function $\boldsymbol{\Phi}_{\boldsymbol{E,i}} : \Omega^\varepsilon \to \mathbb{R}^d$, the pressure $\pi_{E,i} : \Omega^\varepsilon \to \mathbb{R}$:

$$
\left\{
\begin{array}{l}
-\nu \Delta \boldsymbol{\Phi}_{\boldsymbol{E,i}} + \boldsymbol{\nabla} \pi_{E,i} \ \in \ span(\varphi_{\boldsymbol{T_k,1}}, \ldots, \varphi_{\boldsymbol{T_k,r}}) \ in \ T_k \cap \Omega^\varepsilon, \\[2ex]
\operatorname{div} \boldsymbol{\Phi}_{\boldsymbol{E,i}} \ \in \ span(\varpi_{T_k,1}, \ldots, \varpi_{T_k,t}) \ in \ T_k \cap \Omega^\varepsilon, \\[2ex]
\nu \boldsymbol{\nabla} \boldsymbol{\Phi}_{\boldsymbol{E,i}} \boldsymbol{n} - \pi_{E,i} \boldsymbol{n} \ \in \ span(\boldsymbol{\omega}_{\boldsymbol{F,1}}, \ldots, \boldsymbol{\omega}_{\boldsymbol{F,s}}) \ on \ F \cap \Omega^\varepsilon, \ \forall E \in \mathcal{E}(T_k), \\[2ex]
\boldsymbol{\Phi}_{\boldsymbol{E,i}} = \mathbf{0} \ on \ \partial B^\varepsilon \cap T_k, \\[2ex]
\displaystyle\int_{F \cap \partial \Omega^\varepsilon} \boldsymbol{\Phi}_{\boldsymbol{E,i}} \cdot \boldsymbol{\omega}_{\boldsymbol{F,j}} = \left\{ \begin{array}{ll} \delta_{ij}, & F = E \\ 0, & F \neq E \end{array} \right. \quad \forall F \in \mathcal{E}(T_k), \ \forall j = 1, \ldots, s, \\
\displaystyle\int_{T_k \cap \Omega^\varepsilon} \boldsymbol{\Phi}_{\boldsymbol{E,i}} \cdot \varphi_{\boldsymbol{T_k,l}} = 0 \ \forall l = 1, \ldots, r, \\
\displaystyle\int_{T_k \cap \Omega^\varepsilon} \pi_{E,i} \varpi_{T_k,m} = 0 \ \forall m = 1, \ldots, t.
\end{array}
\right.
\tag{21}
$$

■ **Basis functions associated to elements of the coarse mesh**: For each $T \in \mathcal{T}_H$, for $k = 1, \ldots, r$, find $\boldsymbol{\Psi}_{\boldsymbol{T},\boldsymbol{k}} : \Omega^\varepsilon \to \mathbb{R}^d$ and $\pi_{T,k} : \Omega^\varepsilon \to \mathbb{R}$ by solving on T :

$$\begin{cases} -\nu \Delta \boldsymbol{\Psi}_{\boldsymbol{T},\boldsymbol{k}} + \boldsymbol{\nabla} \pi_{T,k} \in span(\boldsymbol{\varphi}_{\boldsymbol{T},\boldsymbol{1}}, \ldots, \boldsymbol{\varphi}_{\boldsymbol{T},\boldsymbol{r}}) \; in \; T \cap \Omega^\varepsilon, \\ \mathrm{div}\, \boldsymbol{\Psi}_{\boldsymbol{T},\boldsymbol{k}} \in span(\varpi_{T,1}, \ldots, \varpi_{T,t}) \; in \; T \cap \Omega^\varepsilon, \\ \nu \boldsymbol{\nabla} \boldsymbol{\Psi}_{\boldsymbol{T},\boldsymbol{k}} \boldsymbol{n} - \pi_{T,k} \boldsymbol{n} \in span(\boldsymbol{\omega}_{\boldsymbol{F},\boldsymbol{1}}, \ldots, \boldsymbol{\omega}_{\boldsymbol{F},\boldsymbol{s}}) \; on \; F \cap \Omega^\varepsilon, \; \forall F \in \mathcal{E}(T), \\ \boldsymbol{\Psi}_{\boldsymbol{T},\boldsymbol{k}} = \boldsymbol{0} \; on \; \partial B^\varepsilon \cap T, \\ \displaystyle\int_{F \cap \partial \Omega^\varepsilon} \boldsymbol{\Psi}_{\boldsymbol{T},\boldsymbol{k}} \cdot \boldsymbol{\omega}_{\boldsymbol{F},\boldsymbol{j}} = 0, \; \forall F \in \mathcal{E}(T), \; \forall j = 1, \ldots, s, \\ \displaystyle\int_{T \cap \Omega^\varepsilon} \boldsymbol{\Psi}_{\boldsymbol{T},\boldsymbol{k}} \cdot \boldsymbol{\varphi}_{\boldsymbol{T}_{\boldsymbol{k}},\boldsymbol{l}} = \delta_{kl} \; \forall l = 1, \ldots, r, \\ \displaystyle\int_{T \cap \Omega^\varepsilon} \pi_{T,k} \varpi_{T,m} = 0 \; \forall m = 1, \ldots, t. \end{cases} \tag{22}$$

Step 4 : Computation of the basis functions

- The well-posedness of the continuous local problems shown in [6];
- We show the well-posedness of the discrete local problems in 2D and 3D (with a particular family of finite elements).

Step 4 : Computation of the basis functions

- The well-posedness of the continuous local problems shown in [6];
- We show the well-posedness of the discrete local problems in 2D and 3D (with a particular family of finite elements).
- Examples of basis functions (in 2D) :

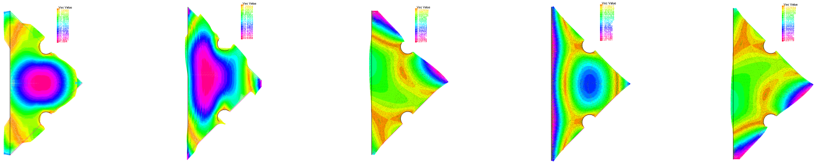

Step 4 : Computation of the basis functions

- The well-posedness of the continuous local problems shown in [6];
- We show the well-posedness of the discrete local problems in 2D and 3D (with a particular family of finite elements).
- Examples of basis functions (in 2D) :

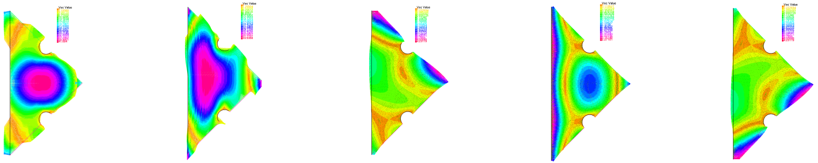

Remark

- No explicit formulation of the basis functions ;
- On triangles without obstacles : $\mathbb{P}_{n+1} \subset V_H$.

Step 5 : Computation of global problem

The coarse-scale formulation of the Stokes problem (2) reads : find $\boldsymbol{u_H} \in V_H$ and $\overline{p}_H \in M_H$ ($:= \mathbb{P}_n^{dc}$) such that :

$$a_H(\boldsymbol{u_H}, \boldsymbol{v}) + b_H(\boldsymbol{v}, \overline{p}_H) = F_H(\boldsymbol{v}), \qquad \forall \boldsymbol{v} \in V_H, \tag{23}$$

$$b_H(\boldsymbol{u_H}, q) = 0, \qquad \forall q \in M_H, \tag{24}$$

$$a_H(\boldsymbol{u_H}, \boldsymbol{v}) = \sum_{T \in \mathcal{T}_H} \int_{T \cap \Omega^\varepsilon} \mu \boldsymbol{\nabla} \boldsymbol{u_H} \cdot \boldsymbol{\nabla} \boldsymbol{v} \quad F_H(\boldsymbol{v}) = \sum_{T \in \mathcal{T}_H} \int_{T \cap \Omega^\varepsilon} \boldsymbol{f} \cdot \boldsymbol{v}$$

$$b_H(\boldsymbol{v}, \overline{p}_H) = -\sum_{T \in \mathcal{T}_H} \int_{T \cap \Omega^\varepsilon} \overline{p}_H \,\mathrm{div}\, \boldsymbol{v}$$

Step 5 : Computation of global problem

The coarse-scale formulation of the Stokes problem (2) reads : find $\boldsymbol{u_H} \in V_H$ and $\overline{p}_H \in M_H$ ($:= \mathbb{P}_n^{dc}$) such that :

$$a_H(\boldsymbol{u_H}, \boldsymbol{v}) + b_H(\boldsymbol{v}, \overline{p}_H) = F_H(\boldsymbol{v}), \qquad \forall \boldsymbol{v} \in V_H, \tag{23}$$

$$b_H(\boldsymbol{u_H}, q) = 0, \qquad \forall q \in M_H, \tag{24}$$

$$a_H(\boldsymbol{u_H}, \boldsymbol{v}) = \sum_{T \in \mathcal{T}_H} \int_{T \cap \Omega^\varepsilon} \mu \boldsymbol{\nabla} \boldsymbol{u_H} \cdot \boldsymbol{\nabla} \boldsymbol{v} \quad F_H(\boldsymbol{v}) = \sum_{T \in \mathcal{T}_H} \int_{T \cap \Omega^\varepsilon} \boldsymbol{f} \cdot \boldsymbol{v}$$

$$b_H(\boldsymbol{v}, \overline{p}_H) = - \sum_{T \in \mathcal{T}_H} \int_{T \cap \Omega^\varepsilon} \overline{p}_H \, \mathrm{div} \, \boldsymbol{v}$$

Theorem (Uniqueness of the discrete global solution)

The Finite Element pair $V_H - \mathbb{P}_n^{dc}$ satisfies the discrete inf-sup condition for the discrete Stokes problem.

Step 6 : Reconstruction of the fine scale solutions

After obtaining the coarse solutions,

$$\boldsymbol{u_H} = (u_{T,1}, \dots, u_{T,r})_{T \in \mathcal{T}_H} \cup (u_{E,1}, \dots, u_{E,s})_{E \in \mathcal{E}_H}$$

$$\overline{p}_H = (\overline{p}_H|_T)_{T \in \mathcal{T}_H}$$

we reconstruct on any coarse element $T \in \mathcal{T}_H$ fine scale solutions by :

$$\boldsymbol{u}_H|_T = \sum_{E \in \mathcal{E}(T)} \sum_{i=1}^{s} u_{E,i} \boldsymbol{\Phi}_{E,i} + \sum_{k=1}^{r} u_{T,k} \boldsymbol{\Psi}_{T,k} \tag{25}$$

$$p_H|_T = \sum_{E \in \mathcal{E}(T)} \sum_{i=1}^{s} u_{E,i} \pi_{E,i} + \sum_{k=1}^{r} u_{T,k} \pi_{T,k} + \overline{p}_H|_T \tag{26}$$

Sommaire

Well posedness of the local problems

Problem

Local problems with **polynomial divergence** and **Lagrange multipliers** $\Longrightarrow$ can not be solved with classical finite element pairs: $\mathcal{P}_2 - \mathcal{P}_1$, $\mathcal{P}_{1nc} - \mathcal{P}_0$, ...

Well posedness of the local problems

Problem

Local problems with **polynomial divergence** and **Lagrange multipliers** $\Longrightarrow$ can not be solved with classical finite element pairs: $\mathcal{P}_2 - \mathcal{P}_1$, $\mathcal{P}_{1nc} - \mathcal{P}_0$, ...

Idea: Use Fortin Lemma

Find a non conforming finite space (V_{n+1}) with the same degrees of freedom that our MsFEM space, i.e

$$\mathcal{N}_j^{f_i} = \int_{f_i} v\mathcal{L}_j(f_i), \quad f_i \in \mathcal{E}_h(\tau)$$

$$\mathcal{N}_j^{\tau} = \int_{\tau} v\mathcal{M}_j(\tau),$$

where the $\mathcal{L}_j(f_i)$ define a basis of $\mathbb{P}_n(f_i)^d$ and the $\mathcal{M}_j(\tau)$ define a basis of $\mathbb{P}_{n-1}(\tau)^d$.

Non-conforming finite element space V_{n+1} of any order in 2D [1]

$$V_{n+1}(\tau) = \mathbb{P}_{n+1}(\tau) + \Sigma_{n+2}(\tau) \tag{27}$$

$$\Sigma_{n+2}(\tau) = span(b_\tau \lambda_1^{n-1-i} \lambda_2^i,\ i = 0, ..., n-1) \subset \mathbb{P}_{n+2}(\tau) \tag{28}$$

where

$$b_\tau = (\lambda_1 - \lambda_2)(\lambda_2 - \lambda_3)(\lambda_3 - \lambda_1) \tag{29}$$

and λ_1, λ_2, λ_3 are the barycentric coordinates of the triangle τ.

[1] Gunar Matthies and Lutz Tobiska. "Inf-sup stable non-conforming finite elements of arbitrary order on triangles". In: *Numerische Mathematik* 102 (Dec. 2005), pp. 293–309. DOI: 10.1007/s00211-005-0648-8

https://github.com/FreeFem/FreeFem-sources/blob/4307d439ca8313cd8fda1c6ce34384e096efea4a/plugin/seq/Element_P2pnc.cpp

https://github.com/FreeFem/FreeFem-sources/blob/4307d439ca8313cd8fda1c6ce34384e096efea4a/plugin/seq/Element_P3pnc.cpp

Non-conforming finite element space V_{n+1} of order 2 and 3 in 3D [2]

$$V_{n+1}(\tau) = \mathbb{P}_{n+1}(T) + \Sigma_{n+2}(\tau) \tag{30}$$

with $\Sigma_{n+2}(\tau) \subset \mathbb{P}_{n+2}(\tau)$ defined for $n = 1$ and $n = 2$ by :

$$\Sigma_3 = \{\lambda_1\lambda_2^2,\ \lambda_1\lambda_3^2,\ \lambda_2\lambda_3^2\}. \tag{31}$$

$$\Sigma_4 = \{\lambda_1^3\lambda_2,\ \lambda_2^3\lambda_3,\ \lambda_3^3\lambda_4,\ \lambda_4^3\lambda_1,\ \lambda_2^3\lambda_1,\ \lambda_1^3\lambda_4,\ \lambda_4^3\lambda_3,\ \lambda_3^3\lambda_2\}. \tag{32}$$

where λ_1, λ_2, λ_3, λ_4 are the barycentric coordinates of the tetrahedron τ.

[2] Balazi Loïc et al. "Inf-sup stable non-conforming finite elements on tetrahedra of order two and order three (in preparation)". In: ()

https://github.com/FreeFem/FreeFem-sources/blob/4307d439ca8313cd8fda1c6ce34384e096efea4a/plugin/seq/Element_P2pnc_3d.cpp

https://github.com/FreeFem/FreeFem-sources/blob/4307d439ca8313cd8fda1c6ce34384e096efea4a/plugin/seq/Element_P3pnc_3d.cpp

Sommaire

Ingredients of the error estimate

Homogenisation Theory

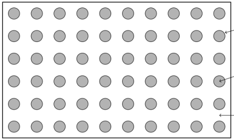

Homogenisation of Stokes flow in porous media : Allaire (1989, 2012), Sanchez-Palencia (1980), Hornung (1997).

Convergence rate : Marusic-Paloka and A. Mikelić (1996), Tartar (1980), Shen (2022).

Ingredients of the error estimate

Homogenisation Theory

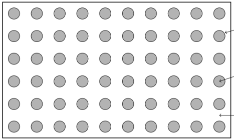

Homogenisation of Stokes flow in porous media : Allaire (1989, 2012), Sanchez-Palencia (1980), Hornung (1997).

Convergence rate : Marusic-Paloka and A. Mikelić (1996), Tartar (1980), Shen (2022).

Ingredients of the error estimate

Homogenisation Theory

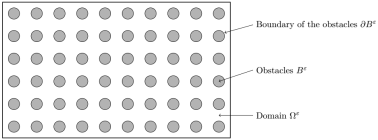

+

Homogenisation of Stokes flow in porous media : Allaire (1989, 2012), Sanchez-Palencia (1980), Hornung (1997).

Convergence rate : Marusic-Paloka and A. Mikelić (1996), Tartar (1980), Shen (2022).

Finite Element Theory

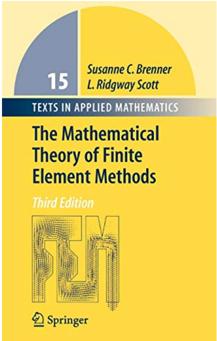

Ingredients of the error estimate

Ingredient 1 : Periodic Homogenisation of the Stokes equations

- Two-scale asymptotic expansions:

$$\boldsymbol{u}_{\boldsymbol{\varepsilon}}(x) = \sum_{k=2}^{+\infty} \varepsilon^k \boldsymbol{u}_k(x, \frac{x}{\varepsilon}) \text{ and } p_\varepsilon(x) = \sum_{k=0}^{+\infty} \varepsilon^k p_k(x, \frac{x}{\varepsilon}) \tag{33}$$

[3] Balazi Loïc, Allaire Grégoire, and Omnes Pascal. "Sharp convergence rates for the homogenization of the Stokes equations in a perforated domain (in preparation)".

Ingredients of the error estimate

Ingredient 1 : Periodic Homogenisation of the Stokes equations

- Two-scale asymptotic expansions:

$$\boldsymbol{u}_{\boldsymbol{\varepsilon}}(x) = \sum_{k=2}^{+\infty} \varepsilon^k \boldsymbol{u}_k(x, \frac{x}{\varepsilon}) \text{ and } p_\varepsilon(x) = \sum_{k=0}^{+\infty} \varepsilon^k p_k(x, \frac{x}{\varepsilon}) \tag{33}$$

- Homogenisation bound (in any dimensions):

Theorem (Homogenisation bounds [3])

Let $\boldsymbol{u}_{\boldsymbol{\varepsilon}}$, p_ε be the solution to the Stokes equations (2), p^* and $\boldsymbol{u}_2$ their homogenizaton approximations. Assuming that $\boldsymbol{f}$ is smooth enough, there exists a constant C, independent of ε and $\boldsymbol{f}$, such that:

$$\begin{aligned} \|p_\varepsilon - p^*\|_{L^2(\Omega^\varepsilon)} &\leq C\varepsilon^{\frac{1}{2}} \|\boldsymbol{f} - \boldsymbol{\nabla} p^*\|_{H^2(\Omega)\cap C^{1,\alpha}(\overline{\Omega})} \\ |\boldsymbol{u}_{\boldsymbol{\varepsilon}} - \varepsilon^2 \boldsymbol{u}_2|_{H^1(\Omega^\varepsilon)} &\leq C\varepsilon^{\frac{3}{2}} \|\boldsymbol{f} - \boldsymbol{\nabla} p^*\|_{H^2(\Omega)\cap C^{1,\alpha}(\overline{\Omega})} \\ \|\boldsymbol{u}_{\boldsymbol{\varepsilon}} - \varepsilon^2 \boldsymbol{u}_2\|_{L^2(\Omega^\varepsilon)} &\leq C\varepsilon^{\frac{5}{2}} \|\boldsymbol{f} - \boldsymbol{\nabla} p^*\|_{H^2(\Omega)\cap C^{1,\alpha}(\overline{\Omega})} \end{aligned} \tag{34}$$

[3] Balazi Loïc, Allaire Grégoire, and Omnes Pascal. "Sharp convergence rates for the homogenization of the Stokes equations in a perforated domain (in preparation)".

Ingredients of the error estimate

Ingredient 2 : Strang Lemma

Lemma (Strang)

Let $\boldsymbol{u_\varepsilon}$ be the exact solution and $\boldsymbol{u_H}$ the approximated solution. Then,

$$\|\boldsymbol{u_\varepsilon} - \boldsymbol{u_H}\|_{V_H} \leq \inf_{\boldsymbol{w_h} \in Z_H} \|\boldsymbol{u_\varepsilon} - \boldsymbol{w_h}\|_{V_H} + \sup_{\boldsymbol{w_h} \in Z_H \setminus \{0\}} \frac{|F_H(\boldsymbol{w_h}) - a_H(\boldsymbol{u_\varepsilon}, \boldsymbol{w_h})|}{\|\boldsymbol{w_h}\|_{V_H}} \tag{35}$$

- Choice of interpolants:

$$\boldsymbol{w_h} = \sum_{E \in \mathcal{E}_H} \sum_{i=1}^{s} \left(\int_{E \cap \partial\Omega^\varepsilon} \boldsymbol{u_\varepsilon} \cdot \boldsymbol{\omega_{E,i}} \right) \boldsymbol{\Phi_{E,i}} + \sum_{T \in \mathcal{T}_H} \sum_{l=1}^{r} \left(\int_{T \cap \Omega^\varepsilon} \boldsymbol{u_\varepsilon} \cdot \boldsymbol{\varphi_{T,l}} \right) \boldsymbol{\Psi_{T,l}} \tag{36}$$

$$q_h = \sum_{E \in \mathcal{E}_H} \sum_{i=1}^{s} \left(\int_{E \cap \partial\Omega^\varepsilon} \boldsymbol{u_\varepsilon} \cdot \boldsymbol{\omega_{E,i}} \right) \pi_{E,i} + \sum_{T \in \mathcal{T}_H} \sum_{l=1}^{r} \left(\int_{T \cap \Omega^\varepsilon} \boldsymbol{u_\varepsilon} \cdot \boldsymbol{\varphi_{T,l}} \right) \pi_{T,l} \tag{37}$$

Main result

Theorem (Error estimate for MsFEM approximation)

The error between the exact solution $(\boldsymbol{u}_{\boldsymbol{\varepsilon}}, p_\varepsilon)$ *to Stokes problem (2) and its MsFEM approximation* $(\boldsymbol{u}_{\boldsymbol{H}}, p_H)$ *is given by :*

$$
\begin{aligned}
&|\boldsymbol{u}_{\boldsymbol{\varepsilon}} - \boldsymbol{u}_{\boldsymbol{H}}|_{H,1} + \varepsilon \|p_\varepsilon - p_H\|_{L^2(\Omega)} \\
&\leq C\varepsilon \left(H^n \|\boldsymbol{f} - \boldsymbol{\nabla} p^*\|_{H^n(\Omega)} + H^n |p^*|_{H^{n+1}(\Omega)} + \left(\sqrt{\varepsilon} + \sqrt{\frac{\varepsilon}{H}} \right) \|\boldsymbol{f} - \boldsymbol{\nabla} p^*\|_{H^2(\Omega) \cap C^1(\overline{\Omega})} \right)
\end{aligned}
$$

where the constant C *depends only on the mesh regularity and the perforation pattern* B^ε*.*

Main result

Theorem (Error estimate for MsFEM approximation)

The error between the exact solution $(\boldsymbol{u_\varepsilon}, p_\varepsilon)$ *to Stokes problem (2) and its MsFEM approximation* $(\boldsymbol{u_H}, p_H)$ *is given by :*

$$
\begin{aligned}
&\left|\boldsymbol{u_\varepsilon} - \boldsymbol{u_H}\right|_{H,1} + \varepsilon \|p_\varepsilon - p_H\|_{L^2(\Omega)} \\
&\leq C\varepsilon \left(H^n \|\boldsymbol{f} - \boldsymbol{\nabla} p^*\|_{H^n(\Omega)} + H^n |p^*|_{H^{n+1}(\Omega)} + \left(\sqrt{\varepsilon} + \sqrt{\frac{\varepsilon}{H}}\right) \|\boldsymbol{f} - \boldsymbol{\nabla} p^*\|_{H^2(\Omega)\cap C^1(\overline{\Omega})} \right)
\end{aligned}
$$

where the constant C *depends only on the mesh regularity and the perforation pattern* B^ε*.*

Remark

The term $\boldsymbol{u_\varepsilon} - \boldsymbol{u_H}$ is of order ε^2. Thus, we note that the estimate for the velocity in the H^1 norm essentially says that the relative error is of the order $\left(H^n + \sqrt{\varepsilon} + \sqrt{\frac{\varepsilon}{H}}\right)$.

Sommaire

Channel flow in perforated domain in 2D

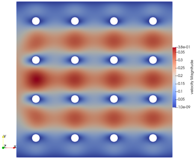

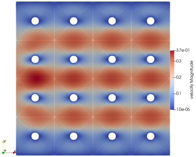

Reference solution (left) compared to MsFEM approximation (right) with 64 coarse elements

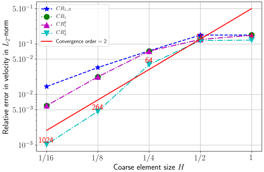

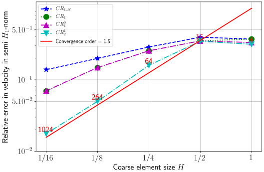

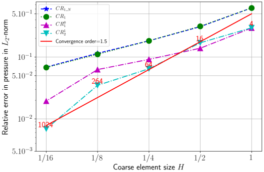

- CR_2^1 MsFEM outperforms the other MsFEMs for both velocity and pressure approximations.
- Comparing CR_1^0 and CR_1 MsFEMs : same behaviours for velocity convergence in norms L_2 and H_1, but a better approximation for the pressure with CR_1^0 MsFEM.
- Comparing CR_{1_N} and CR_1 MsFEM : enriching the face weighting functions improves the velocity approximations.

More complex cases in 2D : Not so clear-cut

We consider a periodic arrangement consisting in 128×128 perforations ($\varepsilon = \frac{1}{128}$) and we take $h = \frac{\varepsilon}{25}$. We compute the MsFEM solutions for $H = \frac{1}{8}, \frac{1}{16}, \frac{1}{32}, \frac{1}{64}$ (256, 1024, 4096, 16384 elements) and we compare with a reference solution.

More complex cases in 2D : Not so clear-cut

We consider a periodic arrangement consisting in 128×128 perforations ($\varepsilon = \frac{1}{128}$) and we take $h = \frac{\varepsilon}{25}$. We compute the MsFEM solutions for $H = \frac{1}{8}, \frac{1}{16}, \frac{1}{32}, \frac{1}{64}$ (256, 1024, 4096, 16384 elements) and we compare with a reference solution.

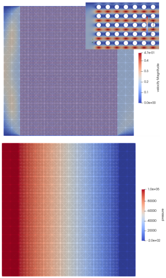

Reference solution

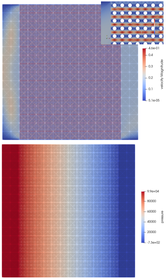

MsFEM CR_1^0 *solution 1024 coarse elements*

More complex cases in 2D : Not so clear-cut

We consider a periodic arrangement consisting in 128×128 perforations ($\varepsilon = \frac{1}{128}$) and we take $h = \frac{\varepsilon}{25}$. We compute the MsFEM solutions for $H = \frac{1}{8}, \frac{1}{16}, \frac{1}{32}, \frac{1}{64}$ (256, 1024, 4096, 16384 elements) and we compare with a reference solution.

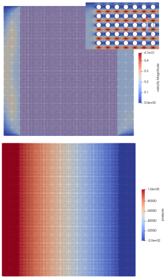

Reference solution

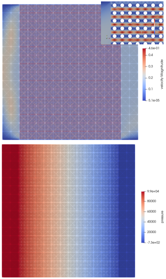

MsFEM CR_1^0 *solution 1024 coarse elements*

- Computation of the reference solution : 1024 CPUs with state of the art preconditionner/solver (cf HPDDM).
- Computation of the MsFEM solutions : less ressources consuming :
  - Computation of basis : about ten minutes per Triangle/CPUs (**reusable**)
  - Computation of the coarse problem : a few minutes on 4 CPUs.
- Visually both solutions look very similar.
- **BUT** : the relative error seems to stagnate for the higher order MsFEM : 10% of error for velocity in norm L_2, 20% of error for velocity in norm H_1 and 5% of error for pressure in norm L_2.

First results in 3D (in non-perforated domain)

We compute the Taylor Green flow and compare with the exact solutions.

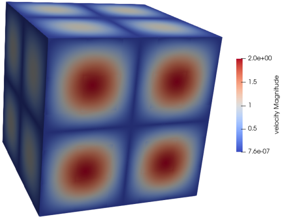

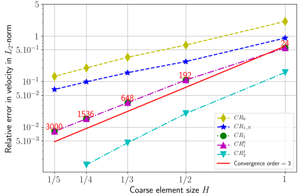

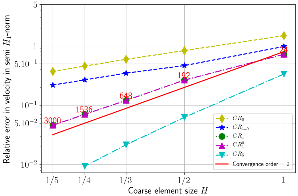

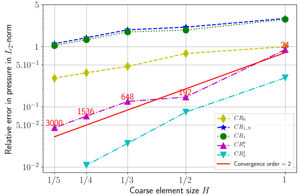

Figures : MsFEM solution computed with 3000 elements with the CR_1^0 method (top left) and convergence rate of the MsFEM solutions for different coarse mesh size H.

Sommaire

Conclusion

Main contributions

- We derived an error estimate for Stokes MsFEM approximation in any dimension ;
- We derived a new family of non-conforming finite element in 3D ;
- We proved the well-posedness of the discrete local problems in 2D and 3D ;
- We implemented 3 new finite elements in FreeFEM source code *(available in version 4.12)* ;
- We implemented the MsFEM in 2D and 3D in FreeFEM for the Stokes and the Oseen equations in a parallel framework.

Conclusion

In progress

- Studying numerically MsFEM in the context of Oseen equations (Petrov-Galerkin formulation, . . .) ;
- Investigating Generalized MsFEM to solve Navier-Stokes equations ;
- Establishing an a posteriori error estimate.

References I

[1] M. Crouzeix and P.-A. Raviart. "Conforming and nonconforming finite element methods for solving the stationary Stokes equations I". en. In: *Revue française d'automatique informatique recherche opérationnelle. Mathématique* 7.R3 (1973), pp. 33–75. ISSN: 0397-9334. DOI: 10.1051/m2an/197307R300331. URL: http://www.esaim-m2an.org/10.1051/m2an/197307R300331 (visited on 11/06/2021).

[2] Weinan E, Bjorn Engquist, and Zhongyi Huang. "Heterogeneous multiscale method: A general methodology for multiscale modeling". In: *Phys. Rev. B* 67 (9 Mar. 2003), p. 092101. DOI: 10.1103/PhysRevB.67.092101. URL: https://link.aps.org/doi/10.1103/PhysRevB.67.092101.

[3] W. E and B. Engquist. "The heterogeneous multiscale methods". In: *Commun. Math. Sci.* 1 (2003), pp. 87–132.

[4] P. Henning and M. Ohlberger. "The heterogeneous multiscale finite element method for elliptic homogenization problems in perforated domains". In: *Numerische Mathematik* 113.4 (2009), pp. 601–629.

[5] Robert Altmann, Patrick Henning, and Daniel Peterseim. "Numerical homogenization beyond scale separation". In: *Acta Numerica* 30 (2021), pp. 1–86. DOI: 10.1017/S0962492921000015.

References II

[6] Qingqing Feng, Gregoire Allaire, and Pascal Omnes. "Enriched Nonconforming Multiscale Finite Element Method for Stokes Flows in Heterogeneous Media Based on High-order Weighting Functions". In: *Multiscale Modeling & Simulation* (Mar. 31, 2022). Publisher: Society for Industrial and Applied Mathematics, pp. 462–492. ISSN: 1540-3459. DOI: 10.1137/21M141926X. URL: https://epubs.siam.org/doi/abs/10.1137/21M141926X (visited on 03/31/2022).

[7] Gunar Matthies and Lutz Tobiska. "Inf-sup stable non-conforming finite elements of arbitrary order on triangles". In: *Numerische Mathematik* 102 (Dec. 2005), pp. 293–309. DOI: 10.1007/s00211-005-0648-8.

[8] Balazi Loïc et al. "Inf-sup stable non-conforming finite elements on tetrahedra of order two and order three (in preparation)". In: ().

[9] Balazi Loïc, Allaire Grégoire, and Omnes Pascal. "Sharp convergence rates for the homogenization of the Stokes equations in a perforated domain (in preparation)". In: ().

Thank You